Impact of Different Parameters on Channel Characteristics in a High-Speed Train Ray Tracing Tunnel Channel Model

Yapei Zhang[1], Yu Liu[1], Jian Sun[1], Cheng-Xiang Wang[2], Xiaohu Ge[3]
[1]Shandong Provincial Key Lab of Wireless Communications, Shandong University, Shandong, 250100, China
[2]School of Engineering and Physical Sciences, Heriot-Watt University, Edinburgh, EH14 4AS, U.K.
[3]Department of Electronics and Information Engineering, Huazhong University of Science and Technology, Wuhan, 430074, China
Email: {ypzhangsdu, xinwenliuyu}@163.com, sunjian@sdu.edu.cn, cheng-xiang.wang@hw.ac.uk, xhge@mail.hust.edu.cn

***Abstract*—In this paper, we investigate the impact of different parameters on channel characteristics in a high-speed train (HST) ray tracing tunnel channel model. Signal propagation in HST tunnel scenarios differs much from that of other HST scenarios due to the unique construction of tunnels. Ray-tracing method is applied to analyze the received power and power delay profile (PDP) of tunnel channel models. Different parameters, i.e., carrier frequency, tunnel shape, tunnel dimension, the distance between the transmitter (Tx) and receiver (Rx), and antenna polarization, are studied via simulation results.**

***Index Terms*—HST, tunnel scenario, ray-tracing method, influencing parameters.**

I. Introduction

HST has attracted more attention recently, and HST communication system will be considered as a typical network for the fifth generation (5G) wireless communications. With an increasing demand for high-capacity and reliable communication networks, HST wireless communication systems have to conquer numerous challenges due to the high speed of train, such as fast handover, large Doppler spreads, high penetration losses, and severe electromagnetic environments. For mitigating these problems, several promising cellular architectures can be adopted, such as distributed antennas (DAS), mobile relay station (MRS), and coordinated multipoint (CoMP) [1].

There are more than 12 scenarios HST may experience in reality [1], such as open space, viaduct, cutting, hilly terrain, tunnels and stations. The first three aforementioned scenarios are the most common ones in HST environments. However, when encountering hill area, the tunnel scenarios will account for majority of transportation. HST tunnels can ensure stable operation and high speed when the train passes through hills. With the limited structure, the length of tunnel can range from several hundred meters to several kilometers depending on surrounding topography. Considering the unique construction, the radio wave propagation inside tunnel scenario is very different from the other HST scenarios [2]. Signals will interact with rich scatterers inside the tunnel. Multiple reflections, diffractions, and transmissions are the dominant propagation mechanisms. To overcome the aforementioned problems, two mainly approaches can permit radio coverage inside tunnel, i.e., leaky feeders and DAS [3]. Although the leaky feeder has been widely used in tunnel communication services, it seems to be too expensive at higher carrier frequencies. Compared with leaky feeders, DAS technology needs lower cost and easy maintenance after system operating. It is more suitable when comes to high frequencies.

For signal propagation in tunnel scenarios, different parameters, such as carrier frequency, tunnel dimension, tunnel cross section shape, curvature, and antenna polarization, have a significant impact on the channel characteristics in tunnels. In [4], influences of different frequencies and different curvatures in the rectangular tunnel were introduced. The study presented in [5] mainly focused on the impact of tunnel diameter on the electromagnetic wave propagation. Effects of antenna polarization modes on relative received power were studied in [6]. Using Wireless InSite software, we have carried out comparisons of channel properties with different parameters in HST tunnels. The comparisons have shown the impact of these parameters in a HST ray tracing tunnel channel model.

The rest of this paper is organized as follows. Ray-tracing channel modeling is introduced in Section II. In Section III, different parameters influencing radio wave propagation inside HST tunnel scenarios are investigated. The corresponding simulation results and analyses are given in Section IV. Finally, the conclusions are drawn in Section V.

II. Ray-Tracing Channel Modeling

A. Ray-Tracing Based Channel Modeling

Ray-tracing method, based on the geometrical optical (GO) theory and the uniform theory of diffraction (UTD), has been widely developed to predict the propagation of high-frequency electromagnetic waves. Ray-tracing channel modeling, which can mimic the multipath of radio rays, is a kind of deterministic channel modeling method with high accuracy. For the facet whose dimension is much larger than the wavelength of the radio ray, the fundamental path loss in tunnels is derived as following [7],

978-1-5090-5932-4/17/$31.00 ©2017 IEEE

$$PL(dB) = 10log_{10}\left[\left(\frac{\lambda}{4\pi}\right)^2\left|\frac{G_T}{L} + \sum_{i=1}^{\infty}\frac{G_i R_i e^{(j\frac{2\pi}{\lambda}(L_i - L))}}{L_i}\right|^2\right] \quad (1)$$

where G_T and G_i are the antenna gains of the Tx and Rx, which related to the path of the direct and the i-th reflected ray, respectively. λ is the free-space wavelength, and R_i denotes the coefficients of all the walls where the i-th ray suffers reflections. L and L_i are path lengths of the direct and the i-th reflected ray, respectively [7]. The received signal is a complex vector superposed of all the rays, and the phases of received rays determine the rays to be added constructively or destructively.

One of the basic procedures of the ray-tracing approach is Shooting and Bouncing Ray (SBR) method. Fig. 1 illustrates the physical interpretation of the SBR method in two dimensional straight tunnel. The transmitter launches rays in all directions, and the radius of a receiver sphere is determined by the path length of a certain ray and by angles between adjacent shot rays [8].

B. Reference Ray-Tracing Model

The straight tunnel model, as shown in Fig. 2, is set as a reference model for comparisons. The cross section of reference model is shown as Tunnel a in Fig. 3. The maximum width and height of the reference model are 5 m and 4.5 m, respectively. The length of this tunnel model is 500 m, and the specific simulation parameters are given in Table I. The origin of coordinates is set at center of tunnel cross section. The Rx is set to move towards Tx along X-axis from 500 m to 1 m.

III. Parameters Influencing Radio Wave Propagation inside HST Tunnel Scenario

In this section, we mainly focus on the parameters influencing radio wave propagation inside HST tunnel scenario, i.e., carrier frequency, tunnel shape, tunnel size, antenna radiation pattern and position, and straight and curved tunnels.

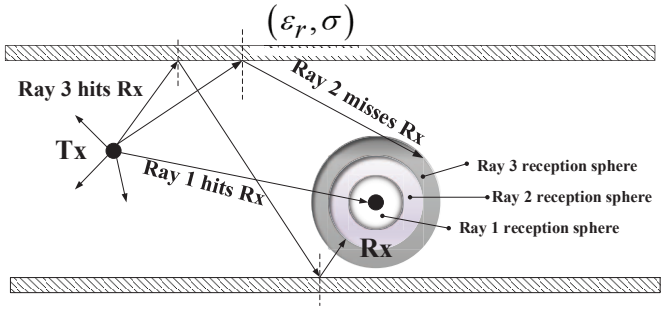

Fig. 1. SBR method in straight tunnel on two dimensions.

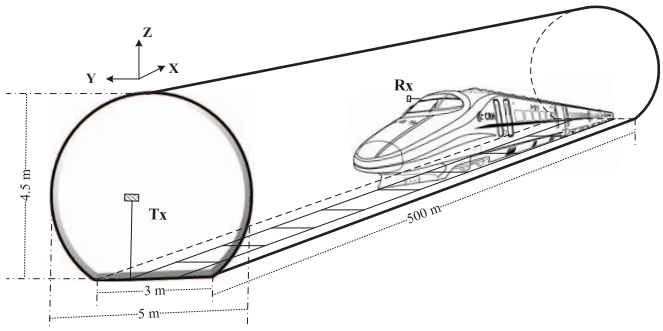

Fig. 2. Reference ray-tracing tunnel model in Wireless InSite.

A. Carrier Frequency and Position

The propagation characteristics of radio wave are dependent on carrier frequencies as well as the distance between the Tx and Rx. In order to highlight their effects, the following equation is given with respect to frequencies and positions in [9],

$$G(d, f) = k\left(\frac{d}{d_0}\right)^{-a}\left(\frac{f}{f_0}\right)^{-b} \quad (2)$$

where G is the path gain (dB), a is the distance exponent, and b is the frequency exponent. d and d_0 denote distance and reference distance, respectively. f and f_0 denote frequency and reference frequency, respectively.

Measurements of path loss with different frequencies were carried out in [10]. In the straight section of the subway tunnel, path loss at 2.45 GHz was 14 dB lower than that at 5.7 GHz on average.

B. Tunnel Shape

There are several typical tunnel shapes in reality, such as arched, rectangular, circular, and semi-circular cross sections in Fig. 3. The arched ones are the most common cross section taking into account the structure and construction of HST tunnel. Tunnel a is the cross section of the reference model in Section II. In [11], the attenuation constant in different tunnels, when carrier frequency is in ultra-high frequency (UHF) segment, has been given as

$$\alpha = k\lambda^2\left[\frac{\varepsilon_r}{w^3\sqrt{\varepsilon_r - 1}} + \frac{1}{h^3\sqrt{\varepsilon_r - 1}}\right] \quad (3)$$

where w and h are the maximum width and height of the tunnel, respectively. ε_r is the dielectric constant of tunnel walls, and k is the coefficient which depends on the specific shape of the tunnel, such as 5.09 for the circular tunnel [11].

C. Tunnel Size

The different widths and heights of tunnels have an impact on the radio wave propagation, which can be proved using (3). The attenuation rate will decrease with the increasing of tunnel width. Measurements in [3] also showed that the wide tunnel (9.8 m $\times$ 6.2 m) has lower attenuation rate than the narrow tunnel (4.8 m $\times$ 5.3 m). The attenuation rates of wide

TABLE I
PARAMETERS OF REFERENCE TUNNEL MODEL.

Tunnel Properties			
Material	**Dielectric Constant**	**Conductivity Loss**	**Thickness**
Concrete	$\varepsilon_r = 15$	$\sigma = 0.015S/m$	0.8 m
Tx			
Location	**Antenna**	**Frequency**	**Transmitting Power**
(1,1,0)	half-wave dipole vertical	2.45 GHz	0 dBm
Rx			
Location	**Antenna**	**Frequency**	**Route Spacing**
(x,0,0)	half-wave dipole vertical	2.45 GHz	1 m
SBR setup			
Ray Spacing	**NO. Reflctions**	**NO. Diffractions**	**NO. Transmissions**
0.25 Ω	10	1	1

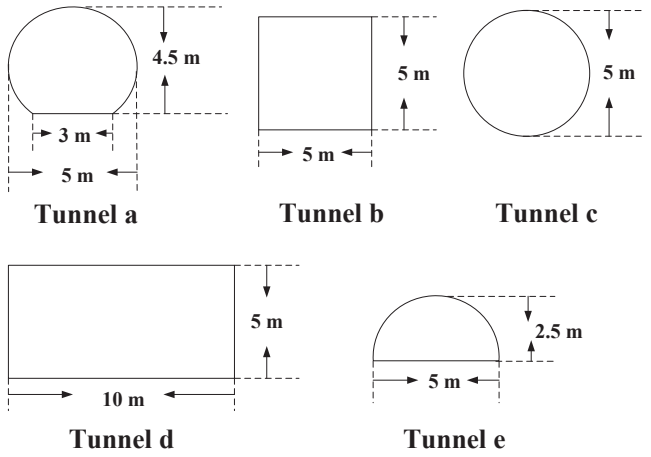

Fig. 3. Typical cross sections for tunnels.

tunnel and narrow tunnel were 69.5 dB/km and 85.9 dB/km, respectively.

D. Antenna Radiation Pattern

Measured results in [9] proved that effects of antenna polarizations are related to different positions. In three scenarios, i.e., narrow tunnel, wide tunnel, and underground mine, vertical polarization resulted in lower path loss than horizontal polarization when the antennas were placed on the wall. The reverse trend could be obtained that the vertical polarization introduced higher path loss when the antennas were placed on the ceiling.

E. Radius of Curvature

The curved cases were investigated in [4], [12]. Simulation results in [4] clearly showed that larger radius of curvature leads to the increasing of attenuation. In [12], the additional attenuation resulted from a curve of length x' can be expressed as

$$L_{\text{curve}}(x') = 10log_{10}\left\lfloor(\rho|\Gamma|)^{2xN_{1c}}\right\rfloor \quad (4)$$

where ρ is the roughness coefficient of the tunnel wall, Γ is the reflection coefficient of each ray, and N_{1c} is the number of reflections per meter which inversed proportional to the linear distance of the curve [12].

IV. SIMULATION RESULTS AND ANALYSES

In this section, the channel characteristics of the proposed reference ray-tracing model with different parameters, such as different carrier frequencies, different cross section shapes, different tunnel dimensions, different positions of receivers, are analyzed and compared. The same properties are used for each simulation expect for the specific compared parameter. Simulation results show that the aforementioned parameters have a significant impact on radio wave propagation.

A. Different Carrier Frequencies

Based on the reference ray-tracing model Tunnel a, simulations are carried out at three different typical carrier frequencies, i.e., 900 MHz, 2.45 GHz, and 5.75 GHz. Standard half-wave dipoles are applied as the Tx and Rx antennas and operate on vertical polarization. The transmitting power is 0 dBm. The transmitter remains fixed and the distance between the Tx and Rx ranges from 500 m to 1 m along X-axis. From Fig. 4, the gap of received power between different frequencies seems to narrow down with the increasing of distance and a highest received power can be seen obviously at 900 MHz. It is caused by the fact that the signal suffers high propagation losses due to shorter wavelength. The channel at 5.75 GHz has severe fast fading than that at 900 MHz and 2.45 GHz. This phenomenon was also dramatized by the measurements at different frequencies in [13].

B. Different Tunnel Shapes

Fig. 5 compares the received power at 2.45 GHz of different tunnel cross sections, i.e., arched tunnel, rectangular tunnel and circular tunnel. The parameters of these three cross sections are illustrated in Fig. 3. From Fig. 5, we can easily notice that the received power in Tunnel c is larger than that in Tunnel a and Tunnel b. In Tunnel a, the fast fading is inconspicuous compared with tunnel b and Tunnel c. Simulation results confirm that the tunnel dimensions have strong impact on the radio wave propagation.

C. Different Tunnel Dimensions

As Fig. 3 shows, Tunnel b is the single-track rectangular tunnel (5 m $\times$ 5 m) and Tunnel d is the double-track rectangular tunnel (10 m $\times$ 5 m). The only difference between Tunnel b and Tunnel d is their widths. The results in Fig. 6 prove that the attenuation rate of received power decreases with the increasing of tunnel dimension, which is consistent with the measurements in [3]. In the near region, the received power in wide tunnel is slightly larger than that in narrow tunnel. The difference of received power turns into obviously with the increasing of distance. Simulation results might conclude stronger waveguide effect in wider tunnel compared to the signal wavelength.

D. Different Receiver Positions and Antenna Polarizations

1) Different receiver positions: By using the parameters in Table I, Fig. 7 shows the PDP at different receiver positions in Tunnel a. The receiver is moving along the X-axis, and the points, i.e., x = 10 m, x = 20 m, and x = 30 m, are chosen for the analyses of PDP. From this figure, we can see when the physical distance between the Tx and Rx increasing, the shift of delay comes to larger, and the attenuation of received power increases. Simulation results confirm that the values of PDP in the tunnel are highly location-dependent.

2) Different antenna polarizations: As Table I illustrates, both the Tx and Rx use half-wave dipoles. For the half-wave dipole, if the antenna polarization is set to vertical, its orientation is along the Z-axis. Selecting horizontal polarization will rotate the antenna about the X-axis by 90 degrees so the antenna will lie along the Y-axis. The comparisons of received power at 2.45 GHz between vertical and horizontal antenna polarization in Tunnel a are illustrated in Fig. 8 and Fig. 9. Fig. 8 shows that the vertical received power has a bit smaller attenuation than the horizontal power when the Tx is mounted on the wall. On the contrary, if the Tx is placed on the ceiling, vertical polarization results in high path loss compared with horizontal case in Fig. 9. The trends generate support from [9].

E. Straight and Curved Tunnels

Fig. 10 exhibits the comparison of received power in straight and curved circular tunnels. The total length is 500 m, the cross section is shown as Tunnel c in Fig. 3, and the radius of curvature is R_{curve} = 300 m. From this figure, we can see a higher received power in straight tunnel. The increasing of curvature enlarges the attenuation of signal. This phenomenon has shown us that the curved case brings more reflections and severe propagation loss.

V. Conclusions

The influences of different parameters (i.e., carrier frequency, tunnel shape, tunnel dimension, receiver position, antenna polarization, and curved tunnel) on propagation characteristics in HST tunnel channel models have been investigated using the Wireless InSite software based on the ray-tracing method. Simulation results have shown that the aforementioned parameters have significant impact on radio wave propagation in tunnels. In general, higher frequencies introduce larger propagation loss and wide tunnels have lower path loss than narrow tunnels. The effect of antenna polarizations on the received power is highly location-dependent. When the Tx is placed on the side of the tunnel wall, vertical polarization antenna has an advantage over the horizontal case in terms of the received power, which is opposite to the case if the Tx is mounted on the ceiling. Moreover, the impact of the curvature is apparent. There are more reflection components in curved tunnels.

Acknowledgment

The authors would like to acknowledge the support from the EU H2020 ITN 5G Wireless project (No. 641985), EU

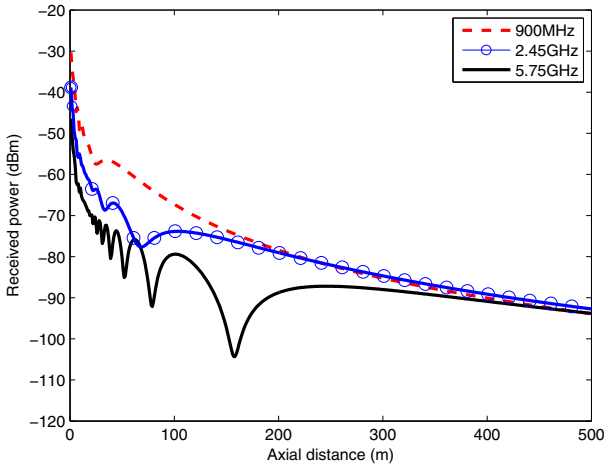

Fig. 4. Received power of different carrier frequencies in Tunnel a.

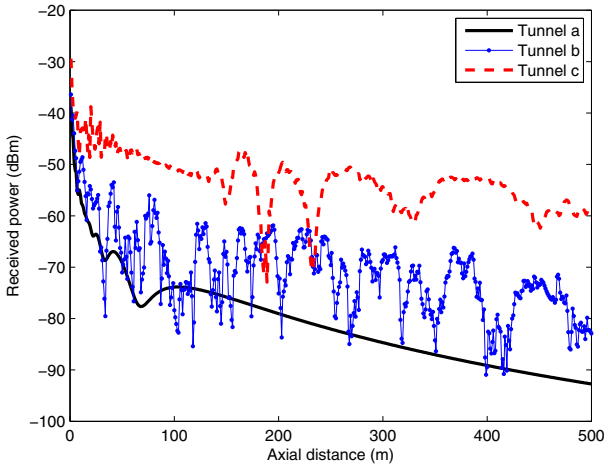

Fig. 5. Received power of different tunnel shapes at 2.45 GHz.

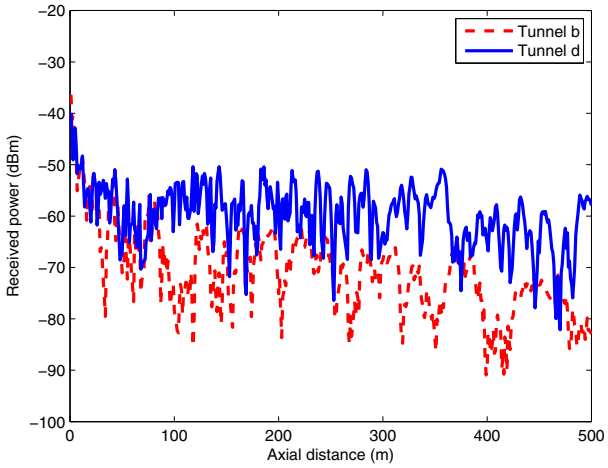

Fig. 6. Received power of different tunnel widths at 2.45 GHz.

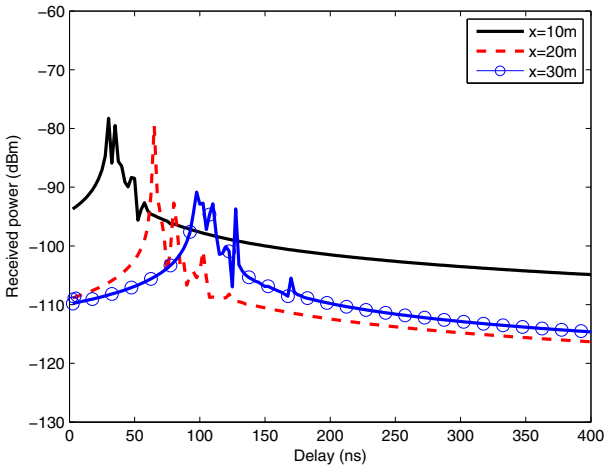

Fig. 7. Power delay profile of different Rx positions in Tunnel a at 2.45 GHz.

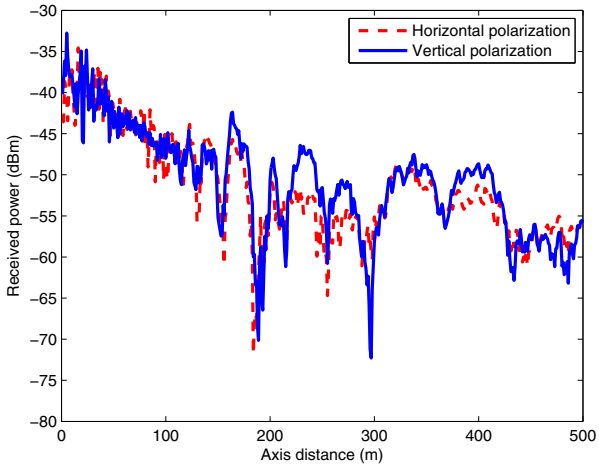

Fig. 8. Received power of different antenna polarization at 2.45 GHz in Tunnel a (placed on tunnel wall).

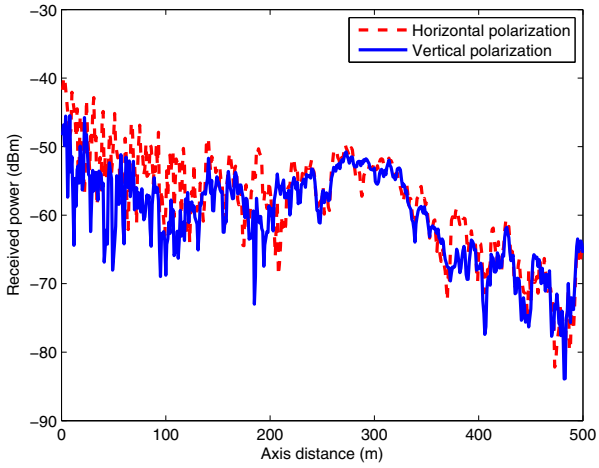

Fig. 9. Received power of different antenna polarization at 2.45 GHz in Tunnel a (placed on tunnel ceiling).

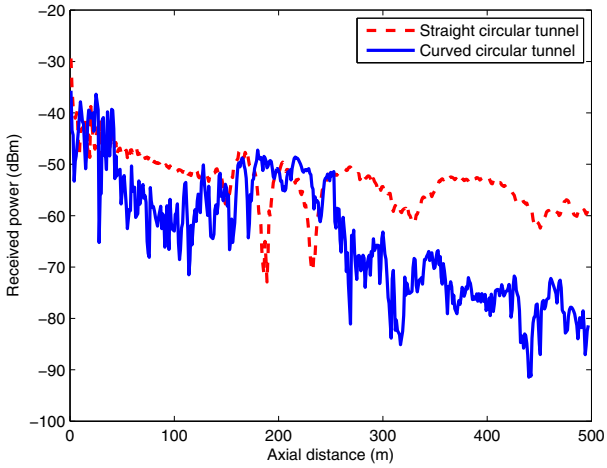

Fig. 10. Received power of straight and curved circular tunnels at 2.45 GHz.

FP7 QUICK project (No. PIRSES-GA-2013-612652), EPSRC TOUCAN project (No. EP/L020009/1), and Natural Science Foundation of China (No. 61210002, 61371110).

REFERENCES

[1] C.-X. Wang, A. Ghazal, B. Ai, P. Fan, and Y. Liu, "Channel measurements and models for high-speed train communication systems: a survey," *IEEE Commun. Surveys Tuts.*, vol. 18, no. 2, pp. 974-987, 2nd Quart., 2016.

[2] Y. Liu, A. Ghazal, C.-X. Wang, X. H. Ge, Y. Yang, and Y. P. Zhang, "Channel measurements and models for high-speed train wireless communication systems in tunnel scenarios," *Sci. China Inf. Sci.*, 2016, accepted for publication.

[3] K. Guan, Z. D. Zhong, J. I. Alonso, and C. Briso-Rodriguez, "Measurement of distributed antenna systems at 2.4GHz in a realistic subway tunnel environment," *IEEE Trans. Veh. Technol.*, vol. 61, no. 2, pp. 834-837, Feb. 2012.

[4] D. G. Dudley, M. Lienard, S. F. Mahmoud, and P. Degauque, "Wireless propagation in tunnels," *IEEE Antennas and Propaga. Mag.*, vol. 49, no. 2, pp. 11–26, Apr. 2007.

[5] J. K. Infantolino, A. J. Kuhlman, M. D. Weiss, and R. L. Haupt, "Modeling RF attenuation in a mine due to tunnel diameter and shape," in *Proc. IEEE APSURSI'13*, Orlando, USA, Jul. 2013, pp. 1914-1915.

[6] J. M. Molina-Garcia-Pardo, M. Lienard, A. Nasr, and P. Degauque, "On the possibility of interpreting field variations and polarization in arched tunnels using a model for propagation in rectangular or circular tunnels," *IEEE Trans. Antennas Propag.*, vol. 56, no. 4, pp. 1206–1211, Apr. 2008.

[7] Y. P. Zhang, "Novel model for propagation loss prediction in tunnels," *IEEE Trans. Veh. Technol.*, vol. 52, no. 5, pp. 1308–1314, Sep. 2003.

[8] A. Hrovat, G. Kandus, and T. Javornik, "A survey of radio propagation modeling for tunnels," *IEEE Commun. Surveys Tuts.*, vol. 16, no. 2, pp. 658–669, May 2014.

[9] S. Bashir, "Effect of antenna position and polarization on UWB propagation channel in underground mines and tunnels," *IEEE Trans. Antennas Propag.*, vol. 62 , no. 9, pp. 4771–4779, Sep. 2014.

[10] J. X. Li, Y. P. Zhao, J. Zhang, R. Jiang, C. Tao, and Z. H. Tan, "Radio channel measurements and analysis at 2.4/5GHz in subway tunnels," *China Commun.*, vol. 12, no. 1, pp. 36–45, Jan. 2015.

[11] C. S. Zhang, and Y. Mao, "Effects of cross section of mine tunnel on the propagation characteristics of UHF radio wave," in *Proc. IEEE ISAPE'06*, Guilin, China, Oct. 2006, pp. 1–5.

[12] C. Briso-Rodriguez, J. M. Cruz, and J. I. Alonso, "Measurements and modeling of distributed antenna systems in railway tunnels," *IEEE Trans. Veh. Technol.*, vol. 56, no. 5, pp. 2870–2879, Sep. 2007.

[13] C. M. Zhou, and J. Waynert, "The equivalence of the ray tracing and modal methods for modeling radio propagation in lossy rectangular tunnels," *IEEE Antennas and Wireless Propaga. Lett.*, vol. 13, no. 1, pp. 615-618, Mar. 2014.